PITX2 Is Involved in Stress Response in Cultured Human Trabecular Meshwork Cells through Regulation of SLC13A3

M. Hermina Strungaru,[1] Tim Footz,[1] Yi Liu,[2] Fred B. Berry,[1,3] Pascal Belleau,[4] Elena V. Semina,[2,5] Vincent Raymond,[4] and Michael A. Walter[1]

Purpose. Mutations of the *PITX2* gene cause Axenfeld-Rieger syndrome (ARS) and glaucoma. In this study, the authors investigated genes directly regulated by the PITX2 transcription factor to gain insight into the mechanisms underlying these disorders.

Methods. RNA from nonpigmented ciliary epithelium cells transfected with hormone-inducible PITX2 and activated by mifepristone was subjected to microarray analyses. Data were analyzed using dCHIP algorithms to detect significant differences in expression. Genes with significantly altered expression in multiple microarray experiments in the presence of activated PITX2 were subjected to in silico and biochemical analyses to validate them as direct regulatory targets. One target gene was further characterized by studying the effect of its knockdown in a cell model of oxidative stress, and its expression in zebrafish embryos was analyzed by in situ hybridization.

Results. Solute carrier family 13 sodium-dependent dicarboxylate transporter member 3 (*SLC13A3*) was identified as 1 of 47 potential PITX2 target genes in ocular cells. PITX2 directly regulates *SLC13A3* expression, as demonstrated by luciferase reporter and chromatin immunoprecipitation assays. Reduction of PITX2 or SLC13A3 levels by small interfering RNA (siRNA)-mediated knockdown augmented the death of transformed human trabecular meshwork cells exposed to hydrogen peroxide. Zebrafish *slc13a3* is expressed in anterior ocular regions in a pattern similar to that of *pitx2*.

Conclusions. The results indicate that *SLC13A3* is a direct downstream target of PITX2 transcriptional regulation and that levels of PITX2 and SLC13A3 modulate responses to oxidative stress in ocular cells. (*Invest Ophthalmol Vis Sci.* 2011;52: 7625–7633) DOI:10.1167/iovs.10-6967

From the Departments of [1]Medical Genetics and [3]Surgery, University of Alberta, Edmonton, Alberta, Canada; [2]Department of Pediatrics and Children's Research Institute, Medical College of Wisconsin and Children's Hospital of Wisconsin, Milwaukee, Wisconsin; [4]Department of Molecular Medicine, Université Laval, Québec City, Quebec, Canada; and [5]Department of Cell Biology, Neurobiology and Anatomy, Medical College of Wisconsin, Milwaukee, Wisconsin.

Supported by the Canadian Institute for Health Research (MAW), Fonds de la Recherche en Santé du Québec (PB, VR), and National Institutes of Health Grant EY015518 (EVS).

Submitted for publication November 29, 2010; revised May 17 and June 2, 2011; accepted June 4, 2011.

Disclosure: **M.H. Strungaru**, None; **T. Footz**, None; **Y. Liu**, None; **F.B. Berry**, None; **P. Belleau**, None; **E.V. Semina**, None; **V. Raymond**, None; **M.A. Walter**, None

Corresponding author: Michael A. Walter, Department of Medical Genetics, University of Alberta, Edmonton, AB, Canada, T6G 2H7; mwalter@ualberta.ca.

The *PITX2* transcription factor was identified as a causative gene for Axenfeld-Rieger syndrome (ARS; Mendelian Inheritance in Man no. 180500) by Semina et al.[1] ARS is a rare autosomal dominant disorder that affects anterior eye development[2] and can occur with or without systemic findings. The ocular findings include structural anomalies of the anterior chamber angle and aqueous drainage structures. Nonocular features typically include facial, dental, and umbilical defects. Our recent study[3] showed that ARS is associated with an approximately 75% risk for glaucoma in patients with *FOXC1* or *PITX2* defects. Glaucoma, the second leading cause of blindness throughout the world,[4–6] is the most important clinical consequence of ARS.[7,8] Glaucoma is often associated with elevated intraocular pressure (IOP), as regulated by the ciliary body (the site of aqueous humor production) and the limbal region (which includes the trabecular meshwork), the principal site of aqueous humor outflow.[4,5] The disease can continue to progress in patients even when IOP is significantly reduced. Research conducted in the past two decades has revealed that oxidative stress is involved in glaucoma pathogenesis.[9–16] Identifying genes involved in adult anterior segment function or responses to oxidative stress will greatly improve our understanding of glaucoma pathology and will result in finding better treatment options.

The PITX2 protein contains a conserved 60 amino acid homeodomain of the paired-bicoid class that is responsible for DNA binding, localization to the nucleus, and protein-protein interaction.[17] Point mutations in *PITX2* have been demonstrated to be loss-of-function mutations affecting DNA binding and transcriptional transactivation.[1,18–27] Tight control of *PITX2* expression is required for normal development of the eye because too much or too little activity of this transcription factor results in anterior segment defects and glaucoma.[24,28] We hypothesize that altered regulation and expression of *PITX2* target genes in adult tissues may have a significant impact on the development and progression of ARS-associated glaucoma and may reveal the cellular pathways affected in primary glaucoma phenotypes.

We previously designed a hormone-inducible transcription factor expression system to discover target genes for *FOXC1*[29] and have now adapted this system to identify *PITX2* target genes in ocular cells. We report here the identification and characterization of the Solute carrier family 13 sodium-dependent dicarboxylate transporter member 3 (*SLC13A3*) as a gene directly regulated by PITX2. Its protein product, NaDC3, is implicated as an important transporter of neuronal metabolites[30] and may regulate the uptake of glutathione (GSH) to protect against ocular oxidative stress.[31] We demonstrate for the first time that PITX2 and SLC13A3 are necessary for cellular responses to oxidative insult from hydrogen peroxide.

METHODS

Plasmids

PITX2-HD-HR. PCR was used to amplify the homeodomain (HD) of wild-type recombinant *PITX2A*.[28] The forward and reverse primers used were 5′-GAT CAT GGG CCC CAA AGG CAG CGG-3′ and 5′-ATG ATC CGG ACC GGG CTC CCT CTT TCT CCA TTT G-3′. The HD fragment was cloned into the pGEM-T vector (Promega, Madison, WI) using the manufacturer's protocol and then subcloned in-frame into *Apa*I/*Rsr*II sites of pcDNAFOXC1-HR[29] (N-terminal Xpresstag; Invitrogen, Burlington, ON, Canada) replacing the forkhead domain.

PITX2-HR. A *Bst*BI site was inserted between amino acids 138 and 139 of recombinant Xpress-PITX2A[28] by site-directed mutagenesis. The hormone-responsive (HR) progesterone receptor binding domain was PCR cloned from the pSWITCH vector (Invitrogen) and then cloned in-frame into the *Bst*BI site.

Xpress-PITX2C. *PITX2C* cDNA was amplified by RT-PCR of human trabecular meshwork RNA (forward, 5′-GAA TTC ATG AAC TGC ATG AAA GGC CCG C-3′; reverse, 5′-CAG GCT CAA GTT ACA CAT AT-3′) and subcloned in-frame into *Eco*RI sites of pCI-HA-PITX2A[32] to replace the isoform A-specific region. The *PITX2C* insert from pCI-HA-PITX2C was subcloned into the *Xba*I/*Eco*RI sites of pcDNA4HisMaxA. Xpress-PITX2C mutants T30P, V45L, and R52C were produced by subcloning the *Xho*I/*Nar*I fragment from pcDNA4HisMax-PITX2A mutant constructs.[27]

SLC13A3 Reporters. Different lengths of the region immediately upstream of the 5′UTR of human *SLC13A3* transcript variant 1 (GenBank accession NM_022829) were PCR amplified from genomic DNA. The primers used for these constructs were −403/+165 (forward, 5′-GCT AGC TCC ACT TTC AGG CTC GAG G-3′; reverse, 5′-CTC GAG GGA GGA GGC GTT ACC TTG G-3′) and −163/+165 (forward, 5′-GCT AGC AGG GAG AGG GCG GGT TCC-3′; reverse, 5′-CTC GAG GGA GGA GGC GTT ACC TTG G-3′). The *SLC13A3* upstream elements were subcloned into vector (pGL3Basic; Promega). Deletion of PITX2 binding site A to generate the −163/+165Δ construct was accomplished using a site-directed mutagenesis kit (QuikChange Lightning; Agilent Technologies, La Jolla, CA) by following the manufacturer's instructions. The forward mutagenesis primer of the complementary pair was 5′-ACC CTC CCC CAG GCT GCG CCG GG-3′.

Plasmid DNA was isolated (Maxiprep or QIAprep Spin Miniprep kits; Qiagen Inc., Mississauga, ON, Canada), and open reading frames were fully sequenced to ensure their integrity.

Cell Culture and Transfection

Human nonpigmented ciliary epithelial (NPCE) and human trabecular meshwork (HTM) cell lines were cultured as described previously.[29] Cells were transfected with plasmid DNA according to the reagent manufacturer's protocols (FuGENE 6 [Roche, Laval, QC, Canada]; or *Trans*IT-LT1 [Mirus Bio LLC, Madison, WI]).

Small interfering RNA (siRNA) specific to the shared region of all isoforms of human *PITX2* was custom ordered from Ambion (Austin, TX) (sense, 5′-CAG CCU GAA UAA CUU GAA Ctt-3′; antisense, 5′-GUU CAA GUU AUU CAG GCU Gtt-3′). siRNA specific to human *SLC13A3* was custom ordered from Thermo Fisher Scientific/Dharmacon (Lafayette, CO) (sense, 5′-GGA GGA AGA AUA AAU CUG AUU-3′; antisense, 5′-UCA GAU UUA UUC UUC CUC CUU-3′). Nontargeting control siRNA (AM4611) was purchased from Ambion. siRNA transfection was performed as described previously[29] according to the reagent manufacturer's protocol (Lipofectamine 2000; Invitrogen).

Hormone-Inducible PITX2 and Microarray Analysis

PITX2-HD-HR and PITX2-HR constructs were transfected into NPCE cells as 2 μg plasmid DNA + 6 μL transfection reagent for 5×10^5 cells/60-mm plate (or 4 μg DNA + 12 μL reagent for 10^6 cells/100-mm plate). Whole-cell protein extracts were derived, and immunoblotting was performed as described previously[27,33] using antibody (anti-Xpress; Invitrogen).

Hormone induction of recombinant PITX2 in NPCE cells with subsequent RNA extraction and microarray analysis was performed as described previously.[29] Statistically significant differences ($P < 0.05$) in the average normalized fluorescence intensity of each transcript between the hormone-inducible constructs and the empty vector samples were determined. Expression data from Affymetrix (Santa Clara, CA) microarrays were first $\log_2$-transformed and then analyzed with dCHIP software.[34,35] Changes in transcript levels were compared among three matched sets of RNA from transfected (empty vector vs. PITX2-HD-HR or PITX2-HR) NPCE cells treated with 100 μg/mL cycloheximide and 10^{-8} M mifepristone. A change in expression was determined to have occurred when at least a 1.5-fold change in expression was detected along with $P < 0.05$ and a present call in 2 of 3 comparisons using Affymetrix software (MAS5).

In Silico Analyses

The in silico tissue expression profile of each gene was determined with an electronic search of the SOURCE database (http://genome-www5.stanford.edu/cgi-bin/source/sourceSearch). The PITX2 DNA binding motif search on the upstream region of genes was performed using RepeatMasker (http://www.repeatmasker.org), Possum (http://zlab.bu.edu/~mfrith/possum), and Ensembl (http://www.ensembl.org/index.html) Web sites and the bicoid binding site matrix (http://www.gene-regulation.com/cgi-bin/pub/databases/transfac/getTF.cgi?AC=M00140). The gene functions were determined using GoSurfer (http://bioinformatics.bioen.uiuc.edu/gosurfer).

Two-Step Quantitative RT-PCR

Total RNA was extracted from siRNA-transfected HTM cells (TRIzol Reagent; Invitrogen). A standard 20 μL reverse transcription reaction contained the following components: 1 μg DNaseI-treated total RNA, 500 ng oligo d(T), 0.5 mM (each) dNTPs, 1× first-strand buffer, 0.01 M dithiothreitol, 40 U RNase inhibitor (RNaseOUT; Invitrogen), and 200 U reverse transcriptase (M-MLV; Invitrogen). Replicate reactions without reverse transcriptase were used as negative controls; 0.5 μL each reaction was used as a template for 10 μL qPCR reactions using a PCR kit (QuantiTect SYBR Green; Qiagen) and the following primer sets: *PITX2* (forward, 5′-AGG CCA CTT TCC AGA GGA AC-3′; reverse, 5′-CGC TCC CTC TTT CTC CAT TT-3′; *SLC13A3* (forward, 5′-GGA CAC TTG CTG GTC AAA GAC-3′; reverse, 5′-ATG GCT CAT GGA CTT GAG TGG-3′); *HPRT1* (forward, 5′-GCC AGA CTT TGT TGG ATT TGA-3′; reverse, 5′-GGC TTT GTA TTT TGC TTT TCC AG-3′). Thermal cycling was performed on a real-time PCR system (7900HT Fast; Applied Biosystems, Carlsbad, CA) with the following conditions: 95°C, 15 minutes; 40 cycles of 94°C, 15 seconds; 60°C, 30 seconds; 72°C, 30 seconds. The relative quantity of gene transcripts (PITX2 siRNA vs. nontargeting siRNA samples), averaged from quadruplicate reactions, was calculated from the equation $2^{-\Delta\Delta Ct}$, with HPRT1 used as the endogenous reference.

Chromatin Immunoprecipitation

Chromatin immunoprecipitation (ChIP) was performed using a ChIP kit (Active Motif ChIP-IT Express; Cedarlane Laboratories Ltd., Burlington, ON, Canada) according to the manufacturer's protocol. NPCE cells were grown to 70% to 80% confluence (~6×10^7 cells) on 100-mm plates. The ChIP reactions were set up by adding protein G magnetic beads, ChIP buffer 1, 6.3 μg sheared chromatin (~300–1000 bp), protease inhibitor cocktail (P8340; Sigma-Aldrich Canada Ltd., Oakville, ON, Canada), and 2 μg of anti-PITX2 antibody (H00005308-M01; Abnova Corporation, Taipei, Taiwan), normal rabbit IgG antibody (10500C; Invitrogen), or anti-acetyl-histone H3 antibody (Lys9; 9671; Cell Signaling Technology, Inc., Danvers, MA). One ChIP reaction did not contain any antibody. A 166-bp fragment in the *SLC13A3* upstream region containing PITX2 binding site B was amplified with the primers 5′-TCC ACT TTC AGG CTC AGA GG-3′ and 5′-GCA GCT GGC TTA TCC

TCT CC-3′. A 243-bp fragment containing PITX2 binding site A was amplified with the primers 5′-AGT GCC TAA CTT TCT CCA ACG-3′ and 5′-CGC TCC ACA CCT TCT TGG-3′. A 277-bp control amplicon from an upstream region lacking predicted PITX2 binding sites was amplified with the primers 5′-TTT GTC TTG CCT GAA TGC TG-3′ and 5′-TGC ACA CTC GTC TCC AAG TC-3′; this fragment was amplified only from genomic DNA and the ChIP input fraction but not from any immunopurified samples.

Transactivation Assays

Transactivation assays were performed as described previously.[27] Transfections were performed in triplicate in NPCE or HTM cells in 24-well plates (4×10^4 cells/15-mm well) using 160 ng empty (pcDNA4HisMax) or Xpress-PITX2C vector, 60 ng pGL3Basic-SLC13A3 luciferase reporter plasmid, 20 ng pCMVβ (Promega) transfection control, and 0.72 μL transfection reagent. Cells were harvested with 100 μL passive lysis buffer (Promega) 48 hours after transfection. Firefly luciferase activity was measured by luminometry (Turner Designs, Sunnyvale, CA) from 10 μL protein lysate mixed with 100 μL luciferase assay reagent (Promega) and was standardized to the β-galactosidase (internal control) activity quantitated by the β-galactosidase enzyme assay system (Promega) from 75 μL protein lysate.

Cell Viability Assay

Cell viability assays were performed with HTM cells (2×10^5 cells/35-mm well) using 2 μg/mL propidium iodide (P4170; Sigma-Aldrich) as described previously.[36] Propidium iodide is excluded by viable cells but penetrates cell membranes of dying or dead cells.

Zebrafish Expression

Zebrafish (*Danio rerio*) were housed in system water on a 14-hour light/10-hour dark cycle; the embryos were acquired by natural spawning and maintained at 28.5°C. The developmental stage was determined by time (hours postfertilization [hpf] or days postfertilization) and morphologic criteria.[37] All experiments were conducted in accordance with the guidelines established by the Institutional Animal Care and Use Committee at the Medical College of Wisconsin, adhering to the ARVO Statement for the Use of Animals in Ophthalmic and Vision Research.

RNA was extracted from zebrafish embryos harvested in reagent (TRIzol; Invitrogen) using standard procedures. cDNA was synthesized from 1 μg total RNA with reverse transcriptase (SuperScript III; Invitrogen) and random hexamers. For RT-PCR analysis of expression, the following *slc13a3* primers were used: forward, 5′-TGG AAA GAC AAG GGA AGG AA-3′; reverse, 5′-ATG GTT GGA AAG AGG CAC AC-3′ (254 bp, encompassing exons 1 and 2). For β-actin control, the following primers were used: forward, 5′-GAG AAG ATC TGG CAT CAC AC-3′; reverse, 5′-ATC AGG TAG TCT GTC AGG TC-3′ (329 bp). For in situ hybridization, a zebrafish *slc13a3* cDNA fragment was PCR amplified using the following primers: forward, 5′-TGC AGC AGA AGC TAA AGC AA-3′; reverse, 5′-CTA AGC CGG ACT CCT CAC AG-3′ (495 bp, encompassing exons 7–11). The resultant fragment was cloned into vector (pCRII-TOPO; Invitrogen), and the insert sequence was verified by direct automated DNA sequencing. Digoxigenin-labeled RNA probes were synthesized by in vitro transcription, and in situ hybridization was performed as previously described.[38]

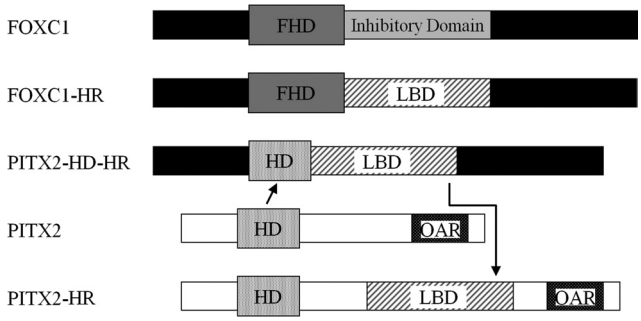

FIGURE 1. Modular construction of the inducible PITX2 constructs. The construct PITX2-HR was created by inserting a truncated form of the hormone-responsive progesterone receptor LBD between the DNA-binding HD and the OAR protein-protein interaction motif. The DNA-binding specificity of the inducible FOXC1-HR construct was altered to be specific for PITX2 by replacing the forkhead domain (FHD) with the PITX2 HD, to create the PITX2-HD-HR construct.

RESULTS

Identification of PITX2 Target Genes by a Hormone-Inducible Expression System

Two hormone-inducible constructs of PITX2 were used in our experiments. In one construct, PITX2-HR, the ligand binding domain (LBD) of the human progesterone receptor was inserted 40 amino acids C-terminal to the homeobox of Xpress-PITX2A (Fig. 1). Another construct, PITX2-HD-HR, replaced the forkhead domain of the FOXC1-HR construct[29] with the PITX2 homeodomain (Fig. 1), thus altering the DNA-binding specificity of the modular protein; in this construct, the LBD replaces the inhibitory domain of the FOXC1 backbone. Both hormone-inducible constructs produced proteins of the appropriate molecular weight in

TABLE 1. Fifteen Genes Regulated by PITX2 That Were Selected for Further Analysis

Gene	Gene Symbol	Function
Coatomer protein complex, subunit gamma 2	*COPG2*	Transport-protein, retrograde Golgi to ER
High-density lipoprotein binding protein (vigilin)	*HDLBP*	RNA binding, nucleic acid binding, lipid transport, and metabolism
Kelch-like 3	*KLHL3*	Protein binding
Nucleoporin 133 kDa	*NUP133*	mRNA export from nucleus, nucleocytoplasmic transport
Poly(ADP-ribose) polymerase family, member 2	*PARP2*	DNA binding, DNA repair, ribosyltransferase activity
Pyruvate dehydrogenase phosphatase isoenzyme 2	*PDP2*	Phosphatase activity, hydrolase activity, catalytic activity, ion binding (Mg)
Phosphatidyl glycerophosphate synthase 1	*PGS1*	Catalytic activity, metabolism
Protein C receptor, endothelial (EPCR)	*PROCR*	Receptor activity, inflammatory response, blood coagulation
Regulating synaptic membrane exocytosis 4	*RIMS4*	Exocytosis activity, neurotransmitter transporter
Solute carrier family 13 member 3	*SLC13A3*	Transport-protein, retrograde Golgi to ER
Tectorin beta	*TECTB*	Transporter activity, ion transporter
Translocase of inner mitochondrial membrane 10 homolog	*TIMM10*	Protein transport
Tolloid-like 2	*TLL2*	Proteolysis, ion binding (Ca, Zn)
Transmembrane protease, serine 2	*TMPRSS2*	Peptidase activity, hydrolase activity, proteolysis, receptor activity
Zinc finger protein 652	*ZNF652*	Nucleic acid binding, zinc ion binding

TABLE 2. Quantitative RT-PCR of HTM Cells Transfected with 100 nM PITX2 siRNA versus Nontargeting Control siRNA

Detector	Average Ct (PITX2 siRNA reaction)	ΔCt (detector vs. HPRT1)	ΔΔCt (PITX2 siRNA vs. control siRNA)	ΔΔCt (SD)	Relative Quantity ($2^{-\Delta\Delta Ct}$)
PITX2	17.77	2.36	1.54	0.57	0.34
SLC13A3	26.12	10.71	1.25	0.86	0.42
HPRT1	15.41	0.00	0.00	0.22	1.00

transfected NPCE cells (Supplementary Data, http://www.iovs.org/lookup/suppl/doi:10.1167/iovs.10-6967/-/DCSupplemental) and, after administration of the progesterone analog mifepristone (RU-486), transactivated the luciferase reporter gene fourfold more than transfection with the empty vector (Supplementary Data, http://www.iovs.org/lookup/suppl/doi:10.1167/iovs.10-6967/-/DCSupplemental). The hormone-inducible expression system was previously used to identify FOXC1 target genes.[29] Mifepristone activated the hormone-inducible constructs, allowing production of mRNA expressed directly in response to PITX2 transcriptional regulation. The addition of cycloheximide eliminated secondary induction events by preventing any new protein from being translated. For controls, NPCE cells were transfected with an empty expression vector and treated in an identical manner with cycloheximide and mifepristone. Total RNA samples collected from three independent experiments were subjected to microarray analysis. The gene expression profile of NPCE cells with induced PITX2 activation was directly compared with that of NPCE cells transfected with the empty vector. The genes differentially expressed by at least 1.5-fold were further analyzed. Analysis of the 45,038 probe set identified 448 genes differentially regulated in response to PITX2-HD-HR and 97 genes differentially regulated in response to PITX2-HR. Forty-seven genes overlapped between the data sets for the two hormone-inducible constructs of PITX2 (Supplementary Data, http://www.iovs.org/lookup/suppl/doi:10.1167/iovs.10-6967/-/DCSupplemental).

SLC13A3 Is a Direct Target Gene of PITX2

The 47 genes with altered expression in the presence of induced PITX2 in multiple microarray experiments were selected for further analysis. The genes were investigated through in silico analyses for expression within the eye and consensus PITX2 DNA-binding sequences (TAATCC, GGATTA, GGCTTAG or CTAAGCC) in the 5′ upstream region of the gene. Fifteen genes with known function, ocular expression, and PITX2 DNA binding sites in the promoter region (Table 1) were subjected to Northern blot analysis or semiquantitative RT-PCR (Supplementary Data, http://www.iovs.org/lookup/suppl/doi:10.1167/iovs.10-6967/-/DCSupplemental). Of these, we chose to further characterize *SLC13A3*, whose mRNA transcript was confirmed by semiquantitative RT-PCR to increase in response to expression of hormone-inducible PITX2A (data not shown). Real-time two-step RT-PCR using HTM cells that were transfected with siRNA showed that a reduction in *PITX2* mRNA to 34% of control levels (all isoforms) led to a reduction of *SLC13A3* transcripts (all isoforms) to 42% of control levels (Table 2). Therefore, PITX2 regulated the expression of *SLC13A3* in both ocular cell lines examined.

The genomic sequence of *SLC13A3* was investigated for putative PITX2 DNA-binding sites using the POSSUM Web site interface. Twelve binding motifs were found in the first 3000 bp upstream of the first exon of *SLC13A3* transcript variant 1. The putative PITX2 DNA-binding site at position −26, site A (Fig. 2), is highly conserved in *Pan troglodytes* (chimpanzee), *Macaca mulatta* (rhesus monkey), and *Canis familiaris* (dog) promoter regions (data not shown). The putative PITX2 DNA binding motif at position −311, site B, is highly conserved only in *P. troglodytes* and *M. mulatta* promoter regions (data not shown). ChIP analysis of NPCE cells was performed to test the direct binding of PITX2 to the *SLC13A3* upstream region. Upstream DNA sequences of *SLC13A3* containing PITX2 binding site A and PITX2 binding site B were amplified by PCR in ChIP samples treated with PITX2 or acetyl-histone H3 (Lys9) antibodies (Fig. 2), indicating the fragments were recovered from PITX2-bound, transcriptionally active chromatin. A negative control region (~20 kb upstream, with no Possum-predicted PITX2 binding sites) was not amplified in any ChIP sample, attesting to the specificity of the antibodies (data not shown).

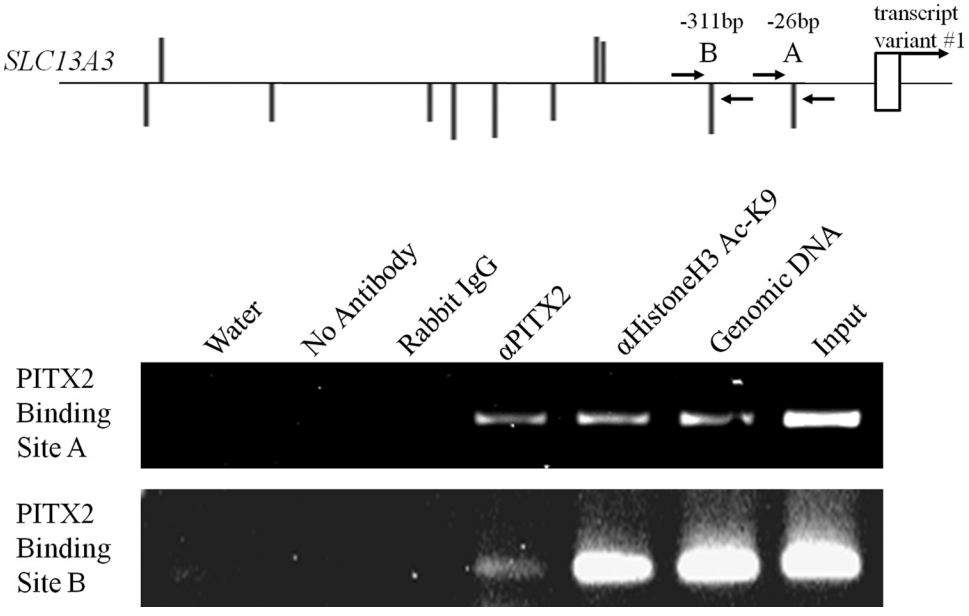

FIGURE 2. PITX2 binds to *SLC13A3* upstream elements. ChIP was used as template for standard PCR. Antibodies against PITX2 and acetyl-histone H3 (Lys9) (positive control for transcriptionally active chromatin) yielded template from which fragments of the SLC13A3 upstream region were amplified, corresponding to putative PITX2 binding sites A and B. ChIP experiments conducted without antibody or with rabbit IgG served as negative controls. All putative PITX2 binding sites upstream of the ATG start codon are represented by *vertical lines*, either above or below the *horizontal line*, corresponding to the forward or reverse orientation, respectively. The length of each line represents the log-likelihood ratio score calculated by POSSUM.

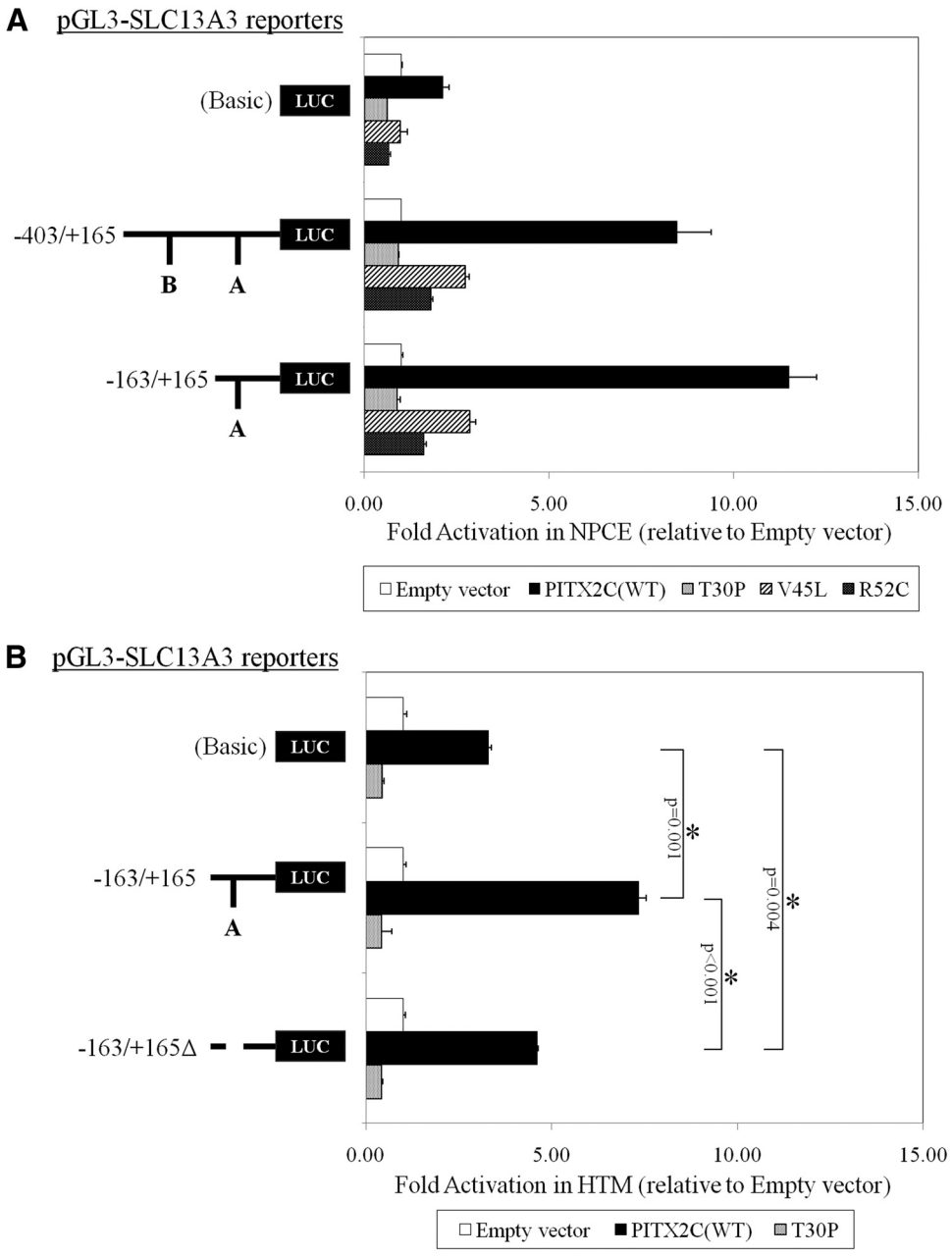

FIGURE 3. Transcriptional transactivation effects of PITX2 on *SLC13A3* upstream elements. Luciferase reporter plasmids (in pGL3Basic) containing different deletion constructs of the *SLC13A3* upstream region were cotransfected in (**A**) NPCE or (**B**) HTM cells with empty pcDNA4 vector, Xpress-PITX2C, or three different ARS-associated homeodomain missense mutations (T30P, V45L, and R52C). Each transfection was performed in triplicate. The error bars represent the relative SEM. $^*P < 0.05$, as calculated with Student's *t*-test.

Activation of the *SLC13A3* upstream region by PITX2 was tested by luciferase reporter assays in NPCE and HTM cells (Fig. 3). The longest construct, −403/+165, included the two putative PITX2 DNA-binding sites, A (5′-TTAAGCCG-3′) and B (5′-TTAATCCT-3′). The second construct, −163/+165, contained only binding site A, whereas −163/+165Δ was deleted for binding site A. Wild-type recombinant PITX2C caused approximately 7- to 12-fold activation of the reporters containing binding site A but was significantly reduced to approximately 4.5-fold when site A was deleted. Activation of the PITX2-responsive reporters was greatly diminished when disease-causing mutant constructs of PITX2C (T30P, V45L, and R52C) were used.

PITX2 and *SLC13A3* Are Involved in a Stress Response Pathway

Recent data indicate that local oxidative stress is a determining factor in the pathology of glaucoma.[13–15] We therefore investigated whether *PITX2* and *SLC13A3* were involved in ocular oxidative stress response pathways. We first tested for cytotoxic concentrations of hydrogen peroxide (200, 400, 600, and 800 μM H_2O_2) on HTM cells; 600 μM H_2O_2 had a significant effect on cell viability (Supplementary Data, http://www.iovs.org/lookup/suppl/doi:10.1167/iovs.10-6967/-/DCSupplemental). Next, we performed cell viability assays to test whether reduction of the PITX2 levels influenced the survival and response to oxidative stress. As shown in Figure 4, when HTM cells were transfected with 100 nM *PITX2* siRNA and exposed to H_2O_2, the number of nonviable HTM cells was significantly increased by at least four times compared with cells treated with nontargeting control siRNA and H_2O_2. We also investigated whether the reduction of *SLC13A3* levels influenced the survival and response to oxidative stress. Transfection of HTM cells with 100 nM *SLC13A3* siRNA caused a 72% reduction in endogenous RNA levels and an 84% reduction in recombinant protein levels (Supplementary Data, http://www.iovs.org/lookup/suppl/doi:10.1167/iovs.10-6967/-/DCSupplemental). We observed a sig-

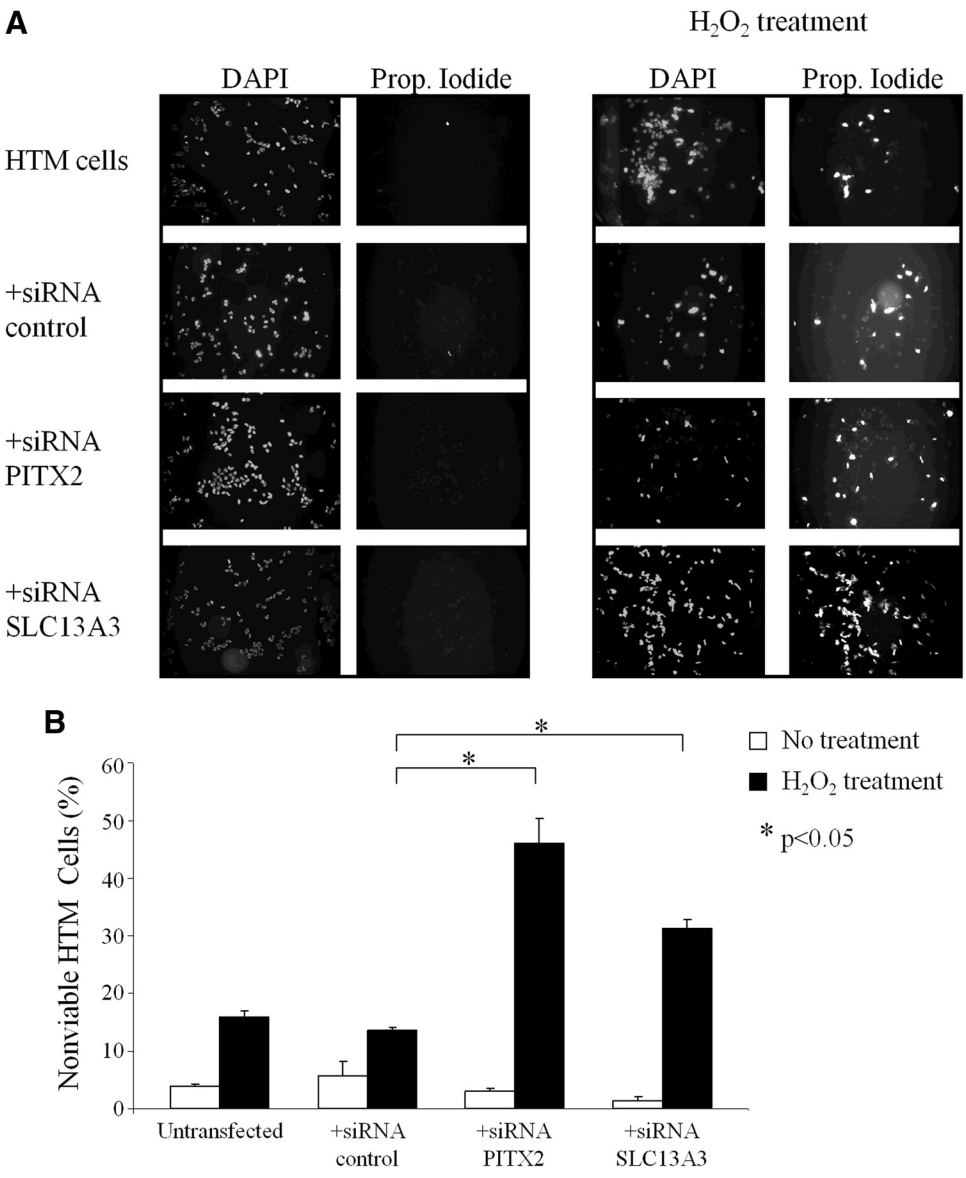

Figure 4. *PITX2* and *SLC13A3* are involved in stress response in HTM cells. HTM cells transfected with 100 nM siRNA were treated 48 hours later with 600 μM H_2O_2, and cell viability was assessed. Nonviable cells were detected by propidium iodide staining 24 hours after H_2O_2 exposure. (**A**) Representative fluorescence photomicrographs of HTM cells, with nuclei counterstained with DAPI. (**B**) Quantification of nonviable cells by counting cells from at least six representative fields. Data are presented as the mean ± the SD from three experiments. $^*P < 0.05$, Student's *t*-test.

nificant twofold reduction in cell viability in H_2O_2-treated HTM cells when they were transfected with *SLC13A3* siRNA compared with nontargeting control siRNA (Fig. 4).

Analysis of *slc13a3* Expression in Zebrafish

We characterized expression of the *slc13a3* homolog in zebrafish (Fig. 5A) to gain a better understanding of its physiological role in relation to the expression of *pitx2*. RT-PCR analysis detected *slc13a3* transcripts in zebrafish embryos starting from 12 hpf (Fig. 5B). Whole mount in situ hybridization detected enrichment for *slc13a3* transcripts in the hatching gland, fins, pharyngeal arches, and periocular mesenchyme at 27 hpf and in the pharynx, kidney, gut, and anterior segment of the eye region in 120 hpf embryos (Fig. 5C). Expression in the developing kidney and gut appeared to be the strongest, particularly at later stages of embryonic development. However, localization of *slc13a3* in anterior ocular regions coincides remarkably with *pitx2* expression during the same developmental stages.[38,39]

Discussion

Mutations in *PITX2* cause ARS, a human autosomal dominantly inherited maldevelopment disorder of the eye associated with glaucoma. How defects in *PITX2* disrupt the developing and mature eye leading to human disease remains unknown. *PITX2* has key roles in the developing eye as *Pitx2*$^{-/-}$ knockout mice present with severe ocular defects, including agenesis of the cornea, abnormal blood vessels, dysgenic optic nerve, and coloboma.[40] However, PITX2 expression is maintained in the adult eye, and recent experiments in the extraocular muscles of mice showed that Pitx2 is also important after birth.[41] Loss of Pitx2 postnatally affected extraocular muscle function, making the extraocular muscles more fatigable than in wild-type mice. Furthermore, glaucoma usually develops in patients with PITX2 defects in their early 20s or 30s (early onset) rather than at birth (congenital). These results indicate that PITX2 is not only important during embryogenesis but is also important for the normal function of the adult eye. We have now identified PITX2 target genes in adult eye cells through the use of a hormone-inducible expression system to elucidate the gene

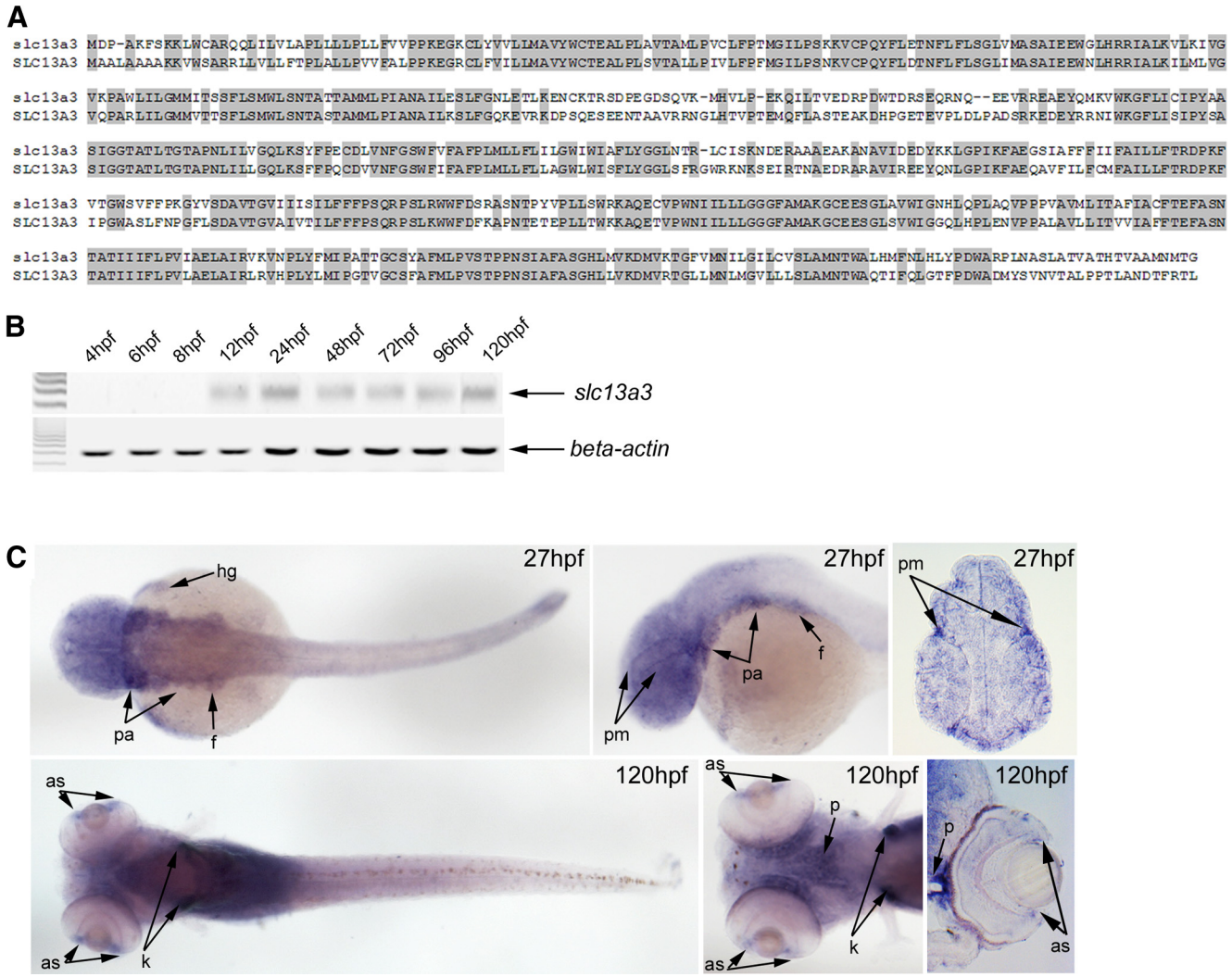

FIGURE 5. Analysis of zebrafish *slc13a3* expression. (**A**) Alignment of zebrafish and human slc13a3/SLC13A3 amino acid sequences (~70% identical). (**B**) Zebrafish *slc13a3* transcript was detected by 12 hpf using RT-PCR. (**C**) In situ hybridization demonstrates expression of the *slc13a3* transcript in whole mount images and transverse sections of zebrafish embryos. hg, hatching gland; pa, pharyngeal arches; f, fin; pm, periocular mesenchyme; as, anterior segment; p, pharynx; k, kidney; hpf, hours postfertilization.

regulatory pathways necessary for normal anterior segment function.

Target genes of PITX2 regulation in different cell types have been identified previously through microarray analyses. Although we did not detect any overlap between muscle-specific genes whose expression correlated with *Pitx2* gene dosage[42] and our data set, two genes from our list of 47 potential direct targets (i.e., *PCDP1/MGC33657* and *TLL2*) were in common with those whose expression in HEK293 cells was altered because of recombinant PITX2 expression.[43] Additional direct target genes of PITX2 regulation have previously been identified, including *PLOD-1*,[44] *Lef-1*,[45] *FoxJ1*,[46] and *Dkk2*,[47] but these were not detected in our microarray experiments. We have extensively characterized physically associated transcription factors in a complex *pitx2-foxc1-foxc2-pawr* regulatory network involved in zebrafish ocular development.[48] The identification here of *SLC13A3* as an ocular target gene of PITX2 provides us with an important tool to monitor the output of modifications to this regulatory network.

Some of the PITX2 target genes identified here (Table 1) have functions relevant to glaucoma pathology. For example, levels of pyruvate dehydrogenase phosphatase (*PDP2*) are decreased in response to the stresses of starvation and diabetes resulting in hyperphosphorylation and inactivation of the pyruvate dehydrogenase complex.[49,50] Our results also show that *SLC13A3* is a direct target of PITX2 regulation. *SLC13A3* encodes a transmembrane protein, NaDC3, that acts as a Na^+/dicarboxylate cotransporter. Mammalian NaDC3 is expressed in the liver, kidney,[51] brain,[52] eye, and optic nerve,[30,53] and here we demonstrate the localization of zebrafish *slc13a3* in similar tissues. Most notably, the pattern of its expression in the periocular mesenchyme and anterior ocular segment at different stages of development overlaps remarkably well with that of zebrafish *pitx2*.[38,39] In situ hybridization of adult mouse eye showed that NaDC3 mRNA is present in anterior and posterior segments. A postulated role of NaDC3 in kidney cells is to transport GSH,[31] one of the main defense mechanisms of the human body against oxidative stress. Aqueous humor of glaucoma patients presents with reduced total antioxidant potential[54] and decreased plasma GSH levels.[55] *SLC13A3* is also hypothesized to contribute to the maintenance of visual function because of its role in transporting the neuronal metabolite N-acetylaspartic acid (NAA) across the plasma membrane in ocular tissues.[30] Mutations in the gene encoding aspartoacylase, which hydrolyses intracellular NAA, cause Canavan disease, an autosomal recessive disorder associated with optic

neuropathy, mental retardation, and brain degeneration.[56] The potential roles of *SLC13A3* in oxidative stress and in the optic neuropathy caused by Canavan disease indicate *SLC13A3* as a good candidate for involvement in glaucoma.

We observed decreased *SLC13A3* expression when endogenous PITX2 levels were reduced and increased *SLC13A3* expression when recombinant PITX2 activity was increased. Molecular analyses indicated that PITX2 (only isoform C was tested) significantly activated transcription from reporter plasmids containing *SLC13A3* upstream elements, whereas PITX2 mutants did not. We also detected binding of endogenous PITX2 to *SLC13A3* promoter region elements through ChIP. *SLC13A3* mRNA is expressed in the ciliary body, the site of aqueous humor production; therefore, the protein encoded by *SLC13A3* might have important functions in the production of aqueous humor. Mutations or downregulation of *SLC13A3* may result in increased IOP and glaucoma.

Our analyses indicate that PITX2 activates genes in the anterior segment of the eye involved in a variety of key processes, including response to cellular stress. Cellular stress can be induced by the generation of reactive oxygen species (ROS), and many experimental studies have shown that local oxidative stress induced by ROS is a determining factor in the pathology of glaucoma. In vitro studies have shown that TM cell morphology is altered on exposure to hydrogen peroxide by compromising cellular integrity and cell adhesion.[14] In addition, aqueous humor drainage from the anterior chamber of the calf eye is affected when TM cells are perfused with hydrogen peroxide.[15] Moreover, it has been shown in humans that TM cells from glaucoma patients presented more oxidative DNA damage than unaffected controls, and this damage is significantly correlated with the elevation of IOP and visual field damage.[13,16] Our studies indicate that reduction in PITX2 protein levels produced an increase in cultured trabecular meshwork cell death when the siRNA-transfected cells were exposed to hydrogen peroxide. Moreover, a reduction in *SLC13A3* also produced an increase in HTM cell death when the cells were exposed to hydrogen peroxide. These results support the hypothesis that *PITX2* acts through *SLC13A3* to modulate responses to cellular stress. We speculate that in healthy adults, PITX2 activates *SLC13A3* whose encoded protein, NaDC3, transports GSH from the aqueous humor into trabecular meshwork cells. GSH would protect the cells against the accumulation of ROS, maintaining normal trabecular meshwork function with normal drainage of aqueous humor and normal IOP. In certain ARS patients we speculate that, in addition to causing the structural defects of anterior segment development, mutations of *PITX2* also cause persistently reduced *SLC13A3* expression resulting in decreased GSH transport into trabecular meshwork cells. As a consequence, a defense mechanism against ROS accumulation is compromised, and, when ROS generation exceeds the cell's antioxidant capacity, ROS cause cell dysfunction and cell death. The number of dead cells will be increased over time, resulting in compromised aqueous humor drainage, elevated IOP, and glaucoma. This biochemical model of glaucoma progression challenges the notion that ARS be classified solely as a secondary form of glaucoma.

In summary, we have identified PITX2 target genes in an NPCE cell line through the use of a hormone-inducible expression system and microarray analysis. This method has now been successfully used to identify genes that are direct targets of transcriptional regulation by either FOXC1[29] or PITX2. As a result we propose that this method can be generally applicable to isolate target genes of transcription factors, depending on the DNA-binding specificity of the construct. Importantly, we have shown that *SLC13A3* is a direct target gene of *PITX2* and that *PITX2* is involved in ocular oxidative cellular stress responses through *SLC13A3*. We have also analyzed the expression of zebrafish *slc13a3* and will be able to monitor its response due to modulation of levels of *pitx2* and other members of its regulatory gene network.

Acknowledgments

The authors thank May Yu for tissue culture expertise.

References

1. Semina EV, Reiter R, Leysens NJ, et al. Cloning and characterization of a novel bicoid-related homeobox transcription factor gene, *RIEG*, involved in Rieger syndrome. *Nat Genet.* 1996;14:392–399.
2. Gould DB, Smith RS, John SW. Anterior segment development relevant to glaucoma. *Int J Dev Biol.* 2004;48:1015–1029.
3. Strungaru MH, Dinu I, Walter MA. Genotype-phenotype correlations in Axenfeld-Rieger malformation and glaucoma patients with FOXC1 and PITX2 mutations. *Invest Ophthalmol Vis Sci.* 2007;48:228–237.
4. Allingham, RR. *Shields' Textbook of Glaucoma*. Philadelphia: Lippincott Williams & Wilkins; 2005:1–2.
5. Gupta D. *Glaucoma Diagnosis and Management*. Philadelphia: Lippincott Williams & Wilkins; 2005:3.
6. Resnikoff, S, Pascolini, D, Etya'ale, D, et al. Global data on visual impairment in the year 2002. *Bull World Health Organ*. 2004;82:844–851.
7. Reese AB, Ellsworth RM. The anterior chamber cleavage syndrome. *Arch Ophthalmol.* 1966;75:307–318.
8. Fitch N, Kaback M. The Axenfeld syndrome and the Rieger syndrome. *J Med Genet.* 1978;15:30–34.
9. Shen F, Chen B, Danias J, et al. Glutamate-induced glutamine synthetase expression in retinal Muller cells after short-term ocular hypertension in the rat. *Invest Ophthalmol Vis Sci.* 2004;45:3107–3112.
10. Galassi F, Renieri G, Sodi A, Ucci F, Vannozzi L, Masini E. Nitric oxide proxies and ocular perfusion pressure in primary open angle glaucoma. *Br J Ophthalmol.* 2004;88:757–760.
11. Chung HS, Harris A, Evans DW, Kagemann L, Garzozi HJ, Martin, B. Vascular aspects in the pathophysiology of glaucomatous optic neuropathy. *Surv Ophthalmol.* 1999;43(suppl 1):S43–S50.
12. Moreno MC, Campanelli J, Sande P, et al. Retinal oxidative stress induced by high intraocular pressure. *Free Radic Biol Med.* 2004;37:803–812.
13. Izzotti A, Sacca SC, Cartiglia C, De Flora S. Oxidative deoxyribonucleic acid damage in the eyes of glaucoma patients. *Am J Med.* 2003;114:638–646.
14. Zhou L, Li Y, Yue BY. Oxidative stress affects cytoskeletal structure and cell-matrix interactions in cells from an ocular tissue: the trabecular meshwork. *J Cell Physiol.* 1999;180:182–189.
15. Kahn MG, Giblin FJ, Epstein DL. Glutathione in calf trabecular meshwork and its relation to aqueous humor outflow facility. *Invest Ophthalmol Vis Sci.* 1983;24:1283–1287.
16. Sacca SC, Pascotto A, Camicione P, Capris P, Izzotti A. Oxidative DNA damage in the human trabecular meshwork: clinical correlation in patients with primary open-angle glaucoma. *Arch Ophthalmol.* 2005;123:458–463.
17. Walter MA. PITs and FOXes in ocular genetics: the Cogan Lecture. *Invest Ophthalmol Vis Sci.* 2003;44:1402–1405.
18. Lines MA, Kozlowski K, Kulak SC, et al. Characterization and prevalence of PITX2 microdeletions and mutations in Axenfeld-Rieger malformations. *Invest Ophthalmol Vis Sci.* 2004;45:828–833.
19. Kulharya AS, Maberry M, Kukolich MK, et al. Interstitial deletions 4q21.1q25 and 4q25q27: phenotypic variability and relation to Rieger anomaly. *Am J Med Genet.* 1995;55:165–170.
20. Alward WL, Semina EV, Kalenak JW, et al. Autosomal dominant iris hypoplasia is caused by a mutation in the Rieger syndrome (*RIEG/PITX2*) gene. *Am J Ophthalmol.* 1998;125:98–100.
21. Kulak SC, Kozlowski K, Semina EV, Pearce WG, Walter MA. Mutation in the *RIEG1* gene in patients with iridogoniodysgenesis syndrome. *Hum Mol Genet.* 1998;7:1113–1117.

22. Saadi I, Semina EV, Amendt BA, et al. Identification of a dominant negative homeodomain mutation in Rieger syndrome. *J Biol Chem.* 2001;276:23034–23041.
23. Perveen R, Lloyd IC, Clayton-Smith J, et al. Phenotypic variability and asymmetry of Rieger syndrome associated with PITX2 mutations. *Invest Ophthalmol Vis Sci.* 2000;41:2456–2460.
24. Priston M, Kozlowski K, Gill D, et al. Functional analyses of two newly identified PITX2 mutants reveal a novel molecular mechanism for Axenfeld-Rieger syndrome. *Hum Mol Genet.* 2001;10: 1631–1638.
25. Phillips JC. Four novel mutations in the *PITX2* gene in patients with Axenfeld-Rieger syndrome. *Ophthalmic Res.* 2002;34:324–326.
26. Borges AS, Susanna R Jr, Carani JC, et al. Genetic analysis of PITX2 and FOXC1 in Rieger Syndrome patients from Brazil. *J Glaucoma.* 2002;11:51–56.
27. Footz T, Idrees F, Acharya M, Kozlowski K, Walter MA. Analysis of mutations of the PITX2 transcription factor found in patients with Axenfeld-Rieger syndrome. *Invest Ophthalmol Vis Sci.* 2009;50: 2599–2606.
28. Kozlowski K, Walter MA. Variation in residual PITX2 activity underlies the phenotypic spectrum of anterior segment developmental disorders. *Hum Mol Genet.* 2000;9:2131–2139.
29. Berry FB, Skarie JM, Mirzayans F, et al. FOXC1 is required for cell viability and resistance to oxidative stress in the eye through the transcriptional regulation of FOXO1A. *Hum Mol Genet.* 2008;17: 490–505.
30. George RL, Huang W, Naggar HA, Smith SB, Ganapathy V. Transport of N-acetylaspartate via murine sodium/dicarboxylate cotransporter NaDC3 and expression of this transporter and aspartoacylase II in ocular tissues in mouse. *Biochim Biophys Acta.* 2004; 1690:63–69.
31. Lash LH. Role of glutathione transport processes in kidney function. *Toxicol Appl Pharmacol.* 2005;204:329–342.
32. Berry FB, Lines MA, Oas JM, et al. Functional interactions between FOXC1 and PITX2 underlie the sensitivity to FOXC1 gene dose in Axenfeld-Rieger syndrome and anterior segment dysgenesis. *Hum Mol Genet.* 2006;15:905–919.
33. Alvarez BV, Vithana EN, Yang Z, et al. Identification and characterization of a novel mutation in the carbonic anhydrase IV gene that causes retinitis pigmentosa. *Invest Ophthalmol Vis Sci.* 2007; 48:3459–3468.
34. Li C, Hung Wong W. Model-based analysis of oligonucleotide arrays: model validation, design issues and standard error application. *Genome Biol.* 2001;2:RESEARCH0032.
35. Li C, Wong WH. Model-based analysis of oligonucleotide arrays: expression index computation and outlier detection. *Proc Natl Acad Sci U S A.* 2001;98:31–36.
36. Yu AL, Fuchshofer R, Kampik A, Welge-Lussen U. Effects of oxidative stress in trabecular meshwork cells are reduced by prostaglandin analogues. *Invest Ophthalmol Vis Sci.* 2008;49:4872–4880.
37. Kimmel CB, Ballard WW, Kimmel SR, Ullmann B, Schilling TF. Stages of embryonic development of the zebrafish. *Dev Dyn.* 1995;203:253–310.
38. Volkmann BA, Zinkevich NS, Mustonen A, et al. Potential novel mechanism for Axenfeld-Rieger syndrome: deletion of a distant region containing regulatory elements of PITX2. *Invest Ophthalmol Vis Sci.* 2011;52:1450–1459.
39. Essner JJ, Branford WW, Zhang J, Yost HJ. Mesendoderm and left-right brain, heart and gut development are differentially regulated by pitx2 isoforms. *Development.* 2000;127:1081–1093.
40. Evans AL, Gage PJ. Expression of the homeobox gene Pitx2 in neural crest is required for optic stalk and ocular anterior segment development. *Hum Mol Genet.* 2005;14:3347–3359.
41. Zhou Y, Cheng G, Dieter L, et al. An altered phenotype in a conditional knockout of Pitx2 in extraocular muscle. *Invest Ophthalmol Vis Sci.* 2009;50:4531–4541.
42. Diehl AG, Zareparsi S, Qian M, Khanna R, Angeles R, Gage PJ. Extraocular muscle morphogenesis and gene expression are regulated by Pitx2 gene dose. *Invest Ophthalmol Vis Sci.* 2006;47: 1785–1793.
43. Huang Y, Huang K, Boskovic G, et al. Proteomic and genomic analysis of PITX2 interacting and regulating networks. *FEBS Lett.* 2009;583:638–642.
44. Hjalt TA, Amendt BA, Murray JC. PITX2 regulates procollagen lysyl hydroxylase (PLOD) gene expression: implications for the pathology of Rieger syndrome. *J Cell Biol.* 2001;152:545–552.
45. Amen M, Liu X, Vadlamudi U, et al. PITX2 and beta-catenin interactions regulate Lef-1 isoform expression. *Mol Cell Biol.* 2007;27: 7560–7573.
46. Venugopalan SR, Amen MA, Wang J, et al. Novel expression and transcriptional regulation of FoxJ1 during oro-facial morphogenesis. *Hum Mol Genet.* 2008;17:3643–3654.
47. Gage PJ, Qian M, Wu D, Rosenberg KI. The canonical Wnt signaling antagonist DKK2 is an essential effector of PITX2 function during normal eye development. *Dev Biol.* 2008;317:310–324.
48. Acharya M, Huang L, Fleisch VC, Allison WT, Walter MA. A complex regulatory network of transcription factors critical for ocular development and disease. *Hum Mol Genet.* 2011;20:1610–1624.
49. Huang B, Wu P, Popov KM, Harris RA. Starvation and diabetes reduce the amount of pyruvate dehydrogenase phosphatase in rat heart and kidney. *Diabetes.* 2003;52:1371–1376.
50. Wu P, Sato J, Zhao Y, Jaskiewicz J, Popov KM, Harris RA. Starvation and diabetes increase the amount of pyruvate dehydrogenase kinase isoenzyme 4 in rat heart. *Biochem J.* 1998;329(pt 1):197–201.
51. Chen X, Tsukaguchi H, Chen XZ, Berger UV, Hediger MA. Molecular and functional analysis of SDCT2, a novel rat sodium-dependent dicarboxylate transporter. *J Clin Invest.* 1999;103:1159–1168.
52. Huang W, Wang H, Kekuda R, et al. Transport of N-acetylaspartate by the Na(+)-dependent high-affinity dicarboxylate transporter NaDC3 and its relevance to the expression of the transporter in the brain. *J Pharmacol Exp Ther.* 2000;295:392–403.
53. Chen XZ, Shayakul C, Berger UV, Tian W, Hediger MA. Characterization of a rat Na+-dicarboxylate cotransporter. *J Biol Chem.* 1998;273:20972–20981.
54. Ferreira SM, Lerner SF, Brunzini R, Evelson PA, Llesuy SF. Oxidative stress markers in aqueous humor of glaucoma patients. *Am J Ophthalmol.* 2004;137:62–69.
55. Gherghel D, Griffiths HR, Hilton EJ, Cunliffe IA, Hosking SL. Systemic reduction in glutathione levels occurs in patients with primary open-angle glaucoma. *Invest Ophthalmol Vis Sci.* 2005;46: 877–883.
56. Matalon R, Michals-Matalon K. Biochemistry and molecular biology of Canavan disease. *Neurochem Res.* 1999;24:507–513.